Chapter 2: Rock-physics Foundation for AVO Analysis

John P. Castagna[1], Satinder Chopra[2], and Firas Al-Jarrah[1]

Introduction

A direct correlation of lithology to stacked and migrated seismic data, although an attractive goal, is usually an elusive one. In extreme cases, such as hard limestone formations encased in clastics, lithologic information may be obvious in the seismic amplitudes. For subsurface formations characterized by small velocity changes between different lithologies, however, such a correlation may not be possible. Similarly, acoustic logs themselves are poor indicators or differentiators of lithology, unless they are combined with other logs such as density or porosity logs. One main reason for this is that reservoir rocks such as sandstone, limestone, and shale each exhibit large acoustic-velocity ranges that may overlap significantly. In addition, this limited information is available only at the location of a well, and seismic data are looked upon to provide it elsewhere. Although the goal of direct correlation from seismic to lithology seems simple, serious thought suggests that it could be a complicated exercise. The seismic response of subsurface rocks depends on the contrasts in compressional- and shear-wave velocities and densities. Those contrasts in turn depend on the rock's lithology, porosity, pore-fluid content, and pressure, all of which affect seismic-wave propagation (e.g., Gregory, 1977; Castagna et al., 1993). That dependence requires knowledge about variations in the elastic properties of rock frames, their mineral constituents, and pore fluids, as well as a model for the interactions among them. Rock physics provides the link between the physical properties of rocks and their seismic response, and that link establishes the P-wave velocity (V_P), S-wave velocity (V_S), and density (ρ) of the subsurface rocks, along with their relationships to the rocks' elastic moduli (bulk modulus κ and shear modulus μ), porosity, pore fluid, temperature, pressure, and the like.

Velocities, densities, and many other physical properties can be measured directly in the laboratory from rock samples taken from boreholes. Such measurements are not available everywhere and may not be directly applicable to in-situ conditions, so empirical relations derived from experiments and well logs are usually applied. Those empirical relations are based on certain data and therefore have assumptions that must be fulfilled before the relations can be applied in a meaningful way. In this chapter, we discuss estimation of rock properties and how they are used to predict a rock's pore-fluid properties and saturation.

Seismic velocities and density

Velocity estimation

The P- and S-wave velocities for homogeneous, nonporous, and isotropic rocks are given, in terms of the elastic constants, by the well-known equations 1 and 2 of Chapter 1 — that is, in terms of the bulk modulus and the shear modulus:

$$V_P = \sqrt{\frac{\kappa + \frac{4}{3}\mu}{\rho}} \quad \text{and} \quad V_S = \sqrt{\frac{\mu}{\rho}}.$$

Both of these equations are derived by assuming the propagation of elastic waves in isotropic elastic media. However, porous media, and therefore porous rocks, are not strictly elastic. For our purposes, we will assume that these equations are applicable, at least to the first order.

The ratio V_P/V_S is an important diagnostic value in seismic determination of lithology, and it can be written as

$$\left(\frac{V_P}{V_S}\right)^2 = \frac{\kappa}{\mu} + \frac{4}{3}. \tag{1}$$

[1]University of Houston, Houston, Texas, U.S.A. Email: jcastagnaou@yahoo.com; firas.jarrah@luminageo.com.
[2]Arcis Seismic Solutions, TGS, Calgary, Alberta, Canada. Email: schopra@arcis.com.

A gas sand thus would show a decrease in V_P (as a result of appreciably lower bulk modulus and somewhat lower density), but only a slight increase in V_S, as a result of a decreasing bulk density. Thus, the ratio V_P/V_S is a good indicator of free gas in the rock's pore space.

The elastic properties of any deformable material body are defined by its elastic moduli. Bulk modulus and shear modulus were defined previously. Here, we define λ another elastic constant, called Lamé's first constant, which is related to the other two as $\kappa = \lambda + 2\mu/3$.

The P-wave velocity can also be written in terms of Lamé's constant:

$$V_P = \sqrt{\frac{\lambda + 2\mu}{\rho}}, \tag{2}$$

where μ is the shear modulus, or second Lamé's constant, and ρ is the density.

Density estimation

The simplest way to compute density is by using the mass-balance equation, given as

$$\rho_{sat} = \rho_m(1 - \phi) + \rho_w S_w \phi + \rho_{hc}(1 - S_w)\phi, \tag{3}$$

where ϕ is porosity, S_w is water saturation, ρ_m is the density of the rock matrix, ρ_{sat} is the density of the saturated rock, ρ_w is the density of saline water or brine, and ρ_{hc} is the density of the hydrocarbon. Here we assume that the average density of the rock matrix is ρ_m and that we have two fluids (water and a hydrocarbon) filling the pores of the rock.

As expected, the density drops for a gas reservoir more rapidly than for an oil reservoir, and that distinction is significant in interpretation of seismic AVO responses. Such observations are apparent on the curves in Figure 1a through 1e, plotted for different values of porosity. In Figure 1f and 1g, we show 3D plots for density variation as a function of water saturation and of porosity, for gas and oil. We note that for a given porosity, density decreases as water saturation decreases. Similarly, density decreases as porosity increases for a given saturation.

The P- and S-wave velocities are affected by factors such as porosity, lithology, saturation, pressure, and temperature, among others.

Factors affecting seismic velocity

As a general tendency, higher-porosity rocks tend to exhibit lower P- and S-wave velocities than do low-porosity rocks. However, velocities depend on a variety of other factors, including lithology, pore shape, fluids (fluid type, saturation, and distribution), effective stress, temperature, frequency, degree of cementation, coordination, grain-contact area and type, and structural arrangement. For example, a low-porosity rock with flat pores may have a lower velocity than a high-porosity rock with the same composition but with spherical pores. That pore-shape dependence is particularly important in rocks with a wide variety of pore-shape distributions, such as carbonates. Generally, velocity-porosity transforms in such formations require extensive local calibration. In granular sedimentary rocks — such as sandstones — velocity-porosity transforms, pore-shape distributions, and other factors may vary more regularly. In such cases, more universal velocity-porosity transforms may be applicable.

A familiar velocity-porosity empirical transform that is used in well-log analysis is the Wyllie et al. (1956, 1958) time-average equation (also known as the volume-average equation), given as

$$\frac{1}{V_P} = \frac{1 - \phi}{V_{P_{ma}}} + \frac{S_w \phi}{V_w} + \frac{(1 - S_w)\phi}{V_{hc}}, \tag{4}$$

where V_P is the P-wave velocity in the saturated rock, $V_{P_{ma}}$ is the P-wave velocity in the matrix (or the grain), V_w is the P-wave velocity in water or brine, V_{hc} is the P-wave velocity in the hydrocarbon, S_w is water saturation, and ϕ is porosity. This equation is often used for determining porosity from well logs for well-consolidated sandstones. In this equation, note that if the matrix velocity and the velocities of brine and hydrocarbon are known, the only other variable in the equation is porosity. As expected, the velocity drops more rapidly for a gas reservoir than for an oil reservoir. That distinction is significant in interpretation of seismic AVO responses.

Wyllie's equation 4 above seems reasonable for clean, well-lithified sandstones that have porosities in the range of 10% to 25%, but it overestimates P-wave velocity at high porosities or low effective stress and for poorly lithified rocks. The Wyllie equation generally does not predict the effect of hydrocarbons correctly and should not be used for that purpose. In view of this, the development of other velocity-porosity transforms has also been reported. Raymer et al. (1980) introduced a modified equation in terms of inverse velocity:

$$V_{P_{sat}} = (1 - \phi)^2 V_{P_{ma}} + \phi V_f, \tag{5}$$

where $V_{P_{ma}}$ is the P-wave velocity in the rock matrix, and V_f is the P-wave velocity in fluid comprising brine and hydrocarbon. This equation is supposed to be valid for lithified sandstones with porosities lower than 37%. In view of the empirical nature of the equation, it may not be valid in all circumstances and may need correction.

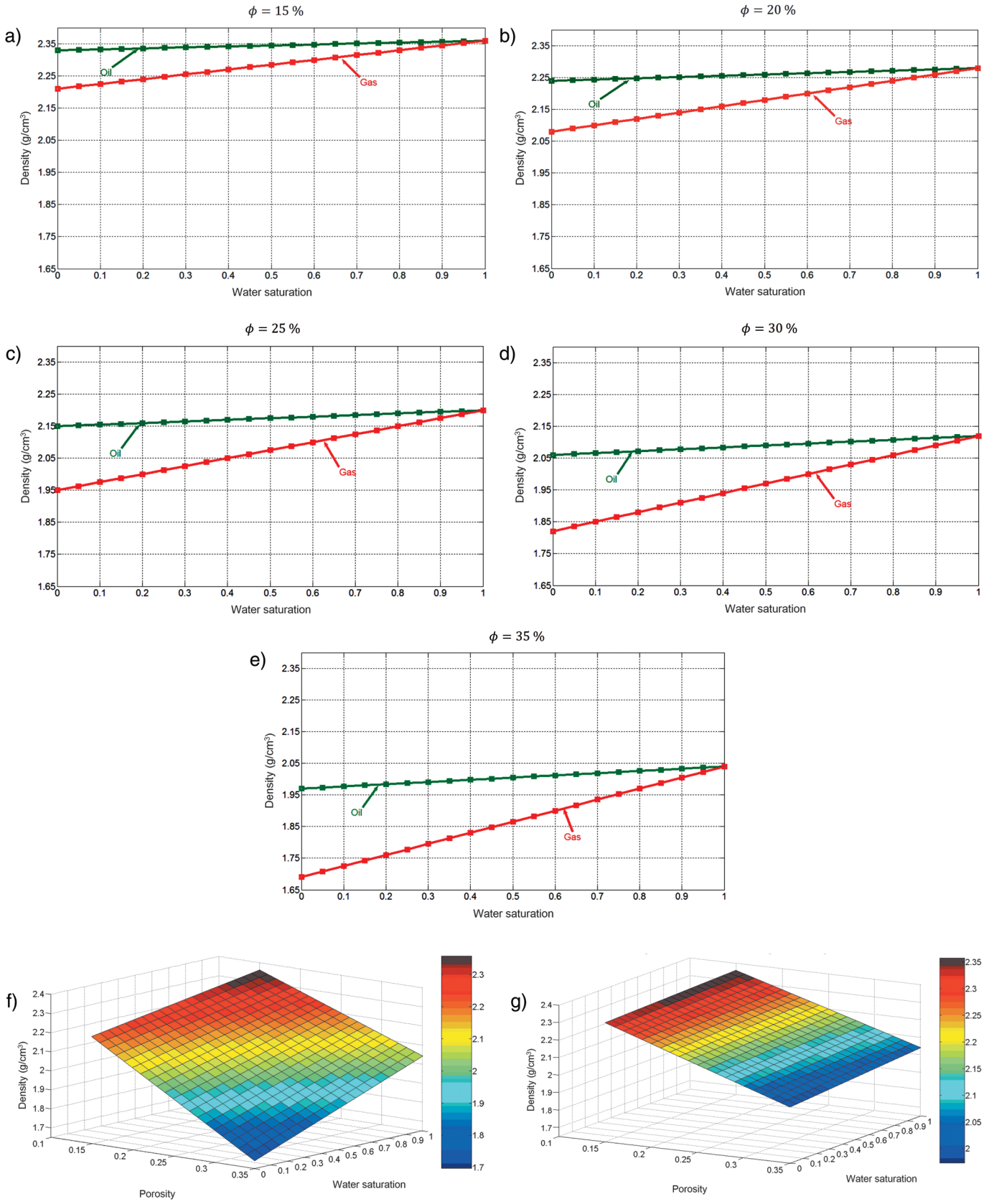

Figure 1. (a through e): Variation of density as a function of water saturation for oil and gas for different values of porosity. (f and g): 3D plots for variation among density, water saturation, and porosity. These graphs indicate that for a gas reservoir, the density drops more rapidly than for an oil reservoir. This distinction is significant in the interpretation of seismic AVO responses.

Similar to the Raymer et al. equation above is the one for S-waves that Castagna (1985) and Castagna et al. (1993) presented:

$$V_S = (1-\phi)^2 V_{S_{ma}}, \quad (6)$$

where $V_{S_{ma}}$ is the shear-wave velocity in the rock matrix.

Notice that in Raymer et al.'s equation 5 above, if V_f is set to zero, equation 6 above for shear waves is obtained. Both Wyllie's time-average equation 4 and Raymer et al.'s equation 5 have a restrictive validity for sandstones, and both equations can overestimate velocities for unconsolidated sandstones, shaly sandstones, and shales.

By measuring velocities at ultrasonic frequencies and as a function of differential pressure and state of saturation, on sandstone samples that had varying porosities and volumes of clay content, Han et al. (1986) suggested the following empirical equations for V_P and V_S:

$$V_P(\text{km/s}) = 5.59 - 6.93\phi - 2.18C, \quad (7)$$

and

$$V_S(\text{km/s}) = 3.52 - 4.91\phi - 1.89C, \quad (8)$$

where ϕ is the porosity and C is the fractional volume of clay content. The above equations are valid for water-saturated sandstones at 40 MPa. The coefficients in the equations change slightly as the confining pressure is varied, although they are stable above 10 MPa.

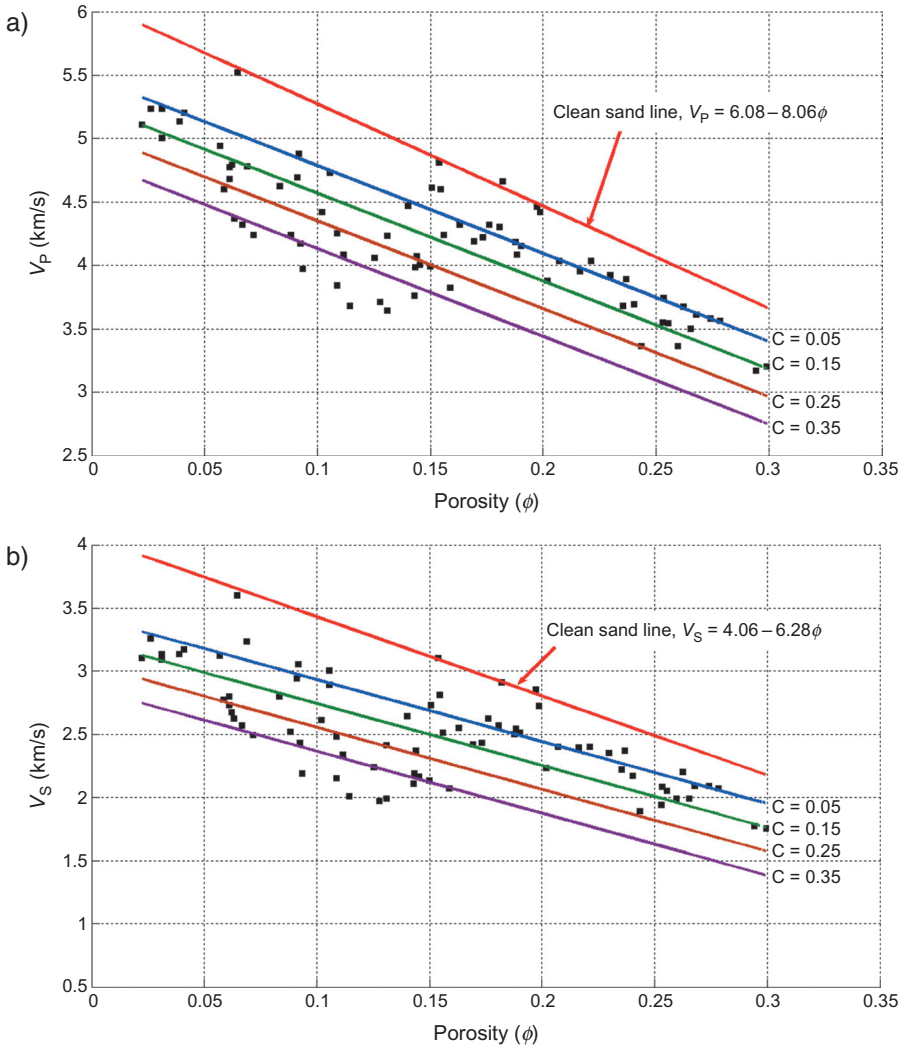

Figure 2. Velocity versus porosity, based on Han et al.'s (1986) empirical relationships for (a) the compressional case and (b) the shear case. Han et al. (1986) found that velocities tend to decrease with an increase in porosity, but they exhibit significant scatter about the regression lines when clay is present (water-saturated). Also, the effects of porosity and clay content are larger on shear velocity than on compressional velocity.

As is seen in Figure 2, Han et al. (1986) found that velocities tend to decrease with an increase in porosity, but they exhibit significant scatter about the regression lines when clay is present (and is water saturated). Also, the effects of porosity and clay content on shear velocity V_S are larger than on compressional velocity V_P. That implies that a sample with high porosity and high clay content tends to have a high V_P/V_S value. If ϕ and C are set equal to zero in the above equations, V_P and V_S are significantly lower than the corresponding velocities for quartz aggregates; i.e., $V_P = 6.05$ km/s and $V_S = 4.09$ km/s. This implies that a small amount of clays (a 1% or 2% volume fraction) can significantly soften the sandstone matrix, thereby yielding reduced velocities. Thus, the clay content in the sandstone should be considered when one is quantifying velocity. Because of the empirical nature of these relationships, the coefficients in the equations could be recalibrated with the available well-log or core data.

Tosaya and Nur (1982) found similar empirical relationships between P-wave velocities and porosity, P-wave velocities and clay content, and S-wave velocities and porosity and clay content. For water-saturated rocks at 40 MPa confining pressure, they found:

$$V_P(\text{km/s}) = 5.8 - 8.6\phi - 2.4C, \quad (9)$$

and

$$V_S(\text{km/s}) = 3.7 - 6.3\phi - 2.1C. \quad (10)$$

Castagna et al. (1985) determined the following empirical equations from well logs for water-saturated samples of shaly sands of the Frio Formation

$$V_P(\text{km/s}) = 5.81 - 9.42\phi - 2.21C \quad (11)$$

and

$$V_S(\text{km/s}) = 3.89 - 7.07\phi - 2.04C. \quad (12)$$

The coefficients are remarkably similar to the results of Tosaya and Nur (1982) and Han (1986), although the rocks and the methods employed were entirely different.

Trends of V_P versus V_S generally are defined more accurately than velocity-porosity trends are, because factors such as porosity, pore shape, and pressure tend to affect V_P and V_S similarly. Pickett (1963) first showed that V_P-V_S trends are well-defined and lithology-dependent (Figure 3). Castagna et al. (1985) and Greenberg and Castagna (1992) followed up on Pickett's work to show that, with global empirical equations, V_S can be predicted with an accuracy of about 5% if lithology and pore-fluid content are known. For mudrocks, Castagna et al. (1985) determined the relationship between V_S and V_P to be

$$V_P(\text{km/s}) = 1.36 + 1.16V_S, \quad (13)$$

which became known as the mudrock equation (Figure 4). Note that this equation is valid for a clastic silicate rock that is composed primarily of clay and silt-size particles. Similar relationships were given for clay shales, limestones, and dolomites (Figure 5).

Xu and White (1995) incorporate pore–aspect ratio information to improve V_S predictions.

These empirical equations provide a framework for AVO analysis (e.g., Smith and Gidlow, 1987; Castagna, 1993; Castagna et al., 1998). For reference, the papers by Goldberg and Gurevich (1998), Greenberg and Castagna (1992), Castagna (1993), and Xu and White (1995) are included on the USB flash drive version of this book.

An exception to reliance on pure empiricism is the fluid-substitution problem, in which Gassmann's theoretical equations (Gassmann, 1951) commonly are applied in practice to predict velocity dependence on pore-fluid properties and saturation. (An English translation of Gassmann's 1951 paper is included on the USB flash drive.) Gassmann's equations are critical for AVO analysis because they define the dominant hydrocarbon signal that AVO is used to detect; that signal is the change in

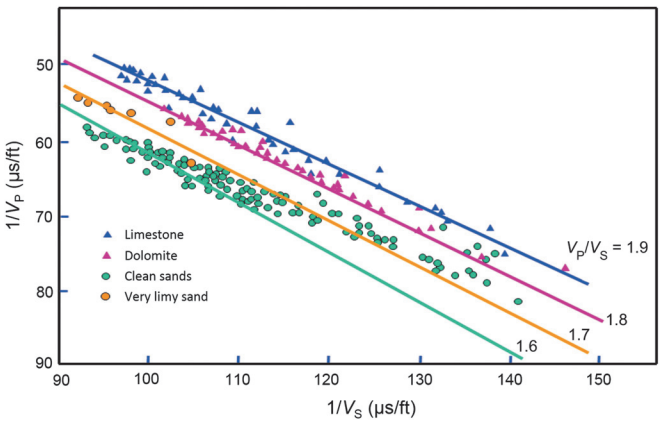

Figure 3. Reciprocal compressional velocity versus reciprocal shear velocity, based on Pickett's laboratory measurements on limestones, dolomites, and sands. After Figure 8 of Pickett (1963). Used by permission.

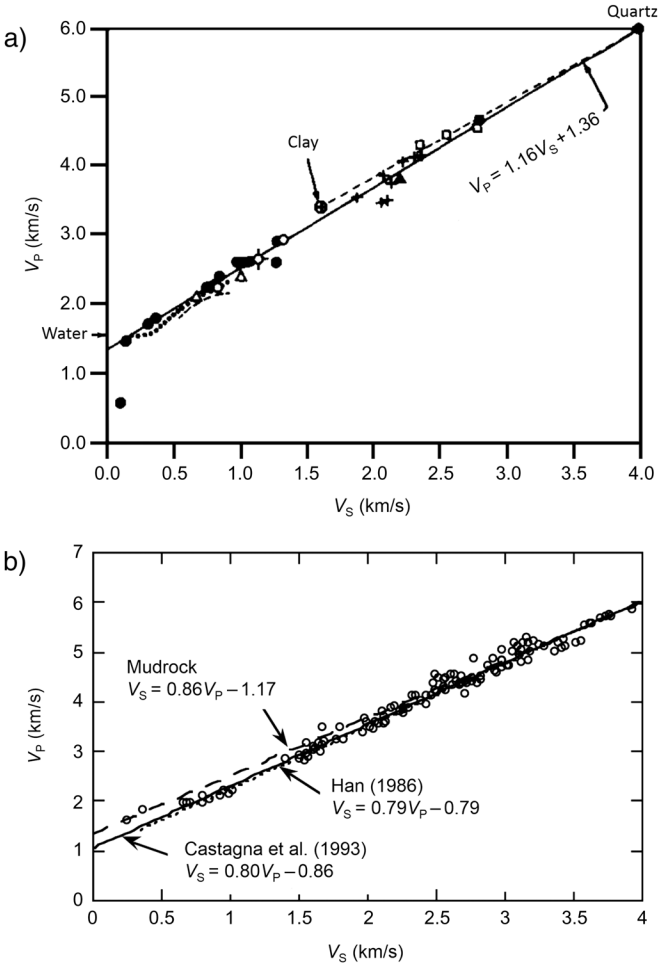

Figure 4. Crossplot of V_P versus V_S for (a) shales and (b) sandstones. The solid line is the linear regression, fitted to the experimental data. After Figure 4 of Castagna et al. (1993). Used by permission.

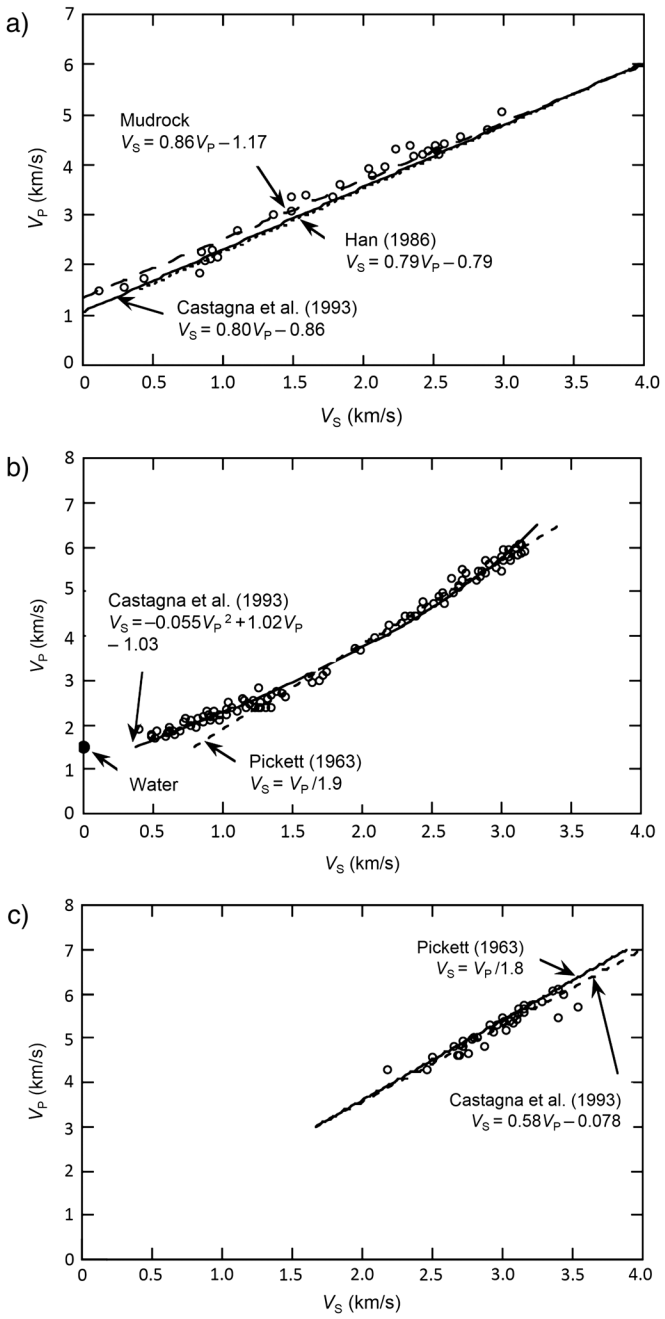

Figure 5. Crossplot of V_P versus V_S for water-saturated (a) shales, (b) limestones, and (c) dolomites. The solid line is the linear regression, fitted to the experimental data. After Figures 3, 5, and 6 of Castagna et al. (1993). Used by permission.

bulk modulus (and thus in V_P) with changes in pore-fluid properties. Given the importance of these equations in AVO analysis, it is perhaps surprising that relatively little attention has been devoted to the nature and implications of Gassmann's results as they relate to AVO analysis. Smith et al. (2003; included on the USB flash drive) provide an excellent review of the rock-physics aspects of the use of Gassmann's equations. Dey et al. (1999) discuss stochastic fluid substitution. Mavko and Mukerji (1998b) investigate the derivation of statistically valid inferences from AVO attribute crossplots, and White and Castagna (2002) perform stochastic fluid-modulus inversion.

The general applicability of Gassmann's equations is probably more limited than most practitioners recognize. We devote the remainder of this chapter to a discussion of the applicability and implications of Gassmann's equations in the context of their use for AVO analysis.

Gassmann's equations

When a seismic wave passes through a porous, saturated rock, the pore fluid contributes to the rock's resistance to compression (i.e., to its incompressibility). The ratio of the applied volumetric stress to the resulting volumetric compression is the bulk modulus, κ. Gassmann's equations mechanically relate the bulk modulus of the saturated rock, κ_{sat}, to the bulk moduli of the pore fluid, κ_f, the nonporous solid material comprising the rock, κ_0, and the porous rock frame, κ^*:

$$\frac{\kappa_{sat}}{\kappa_0 - \kappa_{sat}} = \frac{\kappa^*}{\kappa_0 - \kappa^*} + \frac{\kappa_f}{\phi(\kappa_0 - \kappa_f)} \tag{14}$$

or

$$\kappa_{sat} = \kappa^* + \frac{\left(1 - \frac{\kappa^*}{\kappa_0}\right)^2}{\frac{\phi}{\kappa_f} + \frac{(1-\phi)}{\kappa_0} - \frac{\kappa^*}{\kappa_0^2}}, \tag{15}$$

and

$$\mu^* = \mu_{sat}, \tag{16}$$

where ϕ is the porosity, μ^* is the shear modulus of the rock skeleton, and μ_{sat} is the shear modulus of rock with pore fluid. Equation 14 is elegant in its symmetry and reveals that, for a given frame modulus, the higher the porosity is the smaller the fluid effect will be. This is contrary to the observation that higher porosity rocks have larger fluid effects. The explanation for this apparent discrepancy is that the large fluid effect in high-porosity rocks is entirely the result of the low frame bulk modulus associated with high porosity. (A highly porous but incompressible rock frame has a smaller fluid effect than does a low-porosity but equally incompressible rock frame). From that reasoning, one can conclude that for a given porosity, a low-aspect-ratio pore structure will have a larger fluid effect than do spherical pores. It is worthwhile to point out that equation 14 behaves poorly as porosity approaches zero and as the

frame modulus approaches the solid-grain modulus. Those conditions result in very inaccurate fluid substitutions in low-porosity rocks because small errors in the porosity and other parameters are greatly magnified.

Equation 15 is the standard form (e.g., Domenico, 1976) of the bulk-modulus equation that is used to compute the saturated bulk modulus as the pore-fluid modulus changes, given a known frame bulk modulus, solid-grain modulus, and porosity. It is obvious from an inspection of equation 15 that the maximum fluid-substitution effect occurs when the frame modulus is zero and the saturated modulus is simply the Reuss average of the solid and fluid moduli. We shall see below that the frame bulk modulus can be explicitly excluded from the fluid-substitution calculation.

As Berryman (1999; included on the USB flash drive) pointed out, equation 16 is not an assumption but instead follows from theory.

In the terminology adopted in this paper, we use the broader term "frame modulus" rather than "dry frame modulus," because frame hardening or softening occurs when fluids are changed. Gassmann's equations do not take into account modification of the rock frame properties by the pore fluids. Thus, the frame modulus should be taken as the modulus of the frame in the presence of the wetting fluid. In most cases, the wetting fluid will be brine. Additional complications arise in comparing brine- and hydrocarbon-saturated moduli for the case of oil-wet reservoirs.

Gassmann's assumptions

Gassmann's derivation uses the following seven simplifying assumptions:

1) *As the medium is deformed, there is enough time for the pore pressure to equilibrate throughout the interconnected pore space*. This assumption requires that, for any given frequency, the fluid mobility (permeability/viscosity) is sufficiently high to allow pressure equilibration. That is certainly not a good assumption in low-permeability rocks or in heavy-oil reservoirs. It is commonly assumed that seismic and sonic-log data correspond to the low-frequency region where moduli are virtually the same as they are at the zero-frequency limit, whereas laboratory pulse-transmission-type measurements correspond to the high-frequency regime where moduli are stiffer. Biot's (1956) theory, as made accessible by Geertsma and Smit (1961), is used to perform fluid substitution at laboratory frequencies. Sonic-log data in low-permeability shale-rich or tight-gas sands may not be consistent with Gassmann's equations and may require correction for dispersion (and consequently, for invasion). It is likely that at high frequencies, modulus-versus-saturation curves depend on spatial distribution (Mavko and Mukerji, 1998a), distribution between pore shapes (Endres and Knight, 1997), or some combination thereof. Those effects are smaller at seismic frequencies, where Gassmann's equations are expected to be more applicable. A notable exception would be a finely layered medium of alternating permeable and impermeable layers (sands and shales) with saturation measured for the entire interval. That would occur, for example, in laminated sands in which the layering is finer than the resolution of acoustic logging tools (i.e., when the laminations are much smaller than approximately 1 m). In such a case, saturations need to be distributed to the individual laminations where Gassmann's equations are applied; the interval properties would then be determined by appropriate layer averaging (e.g., Backus, 1962). Less significant for seismic applications, but also of interest, is saturation inhomogeneity within an otherwise uniform, permeable medium (Mavko and Mukerji, 1998a).
2) *All of the pores are in communication*. If there is "acoustically ineffective" isolated porosity (i.e., porosity through which fluids do not flow during passage of the wave), it should be excluded from the porosity used in equation 14 and instead incorporated into the solid-grain modulus (Brown and Korringa, 1975).
3) *The rock frame is chemically and physically inert*. Gassmann's equations are purely mechanical and do not account for changing chemical forces, or for physicochemical changes to the rock frame as fluids are changed, or for pore-pressure changes associated with changing fluid content. It is not uncommon for fluid-saturation changes to be accompanied by pore-pressure changes (e.g., pressure depletion during primary production or pressure increases caused by water or steam injection). If pore pressures drop, the rock frame usually becomes stiffer as a result of consolidation of the pore space. If pore pressure increases, microfractures may open and reduce the frame modulus.
4) *The rock is isotropic and homogeneous*. Gassmann's relations can be readily extended to include anisotropy, but that is not commonly done in practice.
5) *The rock is monomineralic and saturated with a single fluid*. In complex mineralogies, a Hill (1963) or similar average of solid-grain properties is often used. However, if the grain bulk moduli are radically different — particularly if there is a highly compressible solid material such as clay — the physics is much more complex and a simple Hill average will not apply (Berryman and Milton, 1991). Similarly, when there are multiple fluids, Wood's (1941) equation is generally used to compute the effective fluid modulus of the mixture. That equation assumes that the stress in each fluid component

is the same; thus, the strains within the different fluid phases vary greatly. It is not necessarily clear that that must be the case if there is a nonuniform distribution of fluids inside a complex pore space of highly variable pore shapes. It is likelier that some variation of stress occurs within fluid components at different locations in the pore space (which again violates Gassmann's assumption of pressure equilibration), and that this should result in a more uniform distribution of strains and therefore a stiffer modulus than is given by Wood's equation (Castagna and Hooper, 2000). The question has not been completely resolved and must be viewed as an area of ongoing research.

6) *There is no cavitation, and the pore fluid remains coupled to the solid material*. This is probably a good assumption.
7) *The rock system is closed; there is no fluid flow in or out of the rock*. The validity of this assumption at all locations in situ seems perilous.

A common misconception is that Gassmann's equations require spherically shaped pores. That misconception arises from the fact that crack-inclusion models such as that of Kuster and Toksöz (1974) agree with Gassmann's equations only for spherical pores. The limitation occurs because such models assume a situation of isolated pores and do not allow pressures to equilibrate throughout the pore space. Different pore shapes undergo differing degrees of deformation, and thus the pores will have different pore pressures if they are isolated, thereby violating Gassmann's pore-pressure-equilibration assumption. However, spherical pores are all compressed to the same degree, have the same pore pressure, and thus obey Gassmann's assumptions. Nonspherical pores are also valid within Gassmann's assumptions, though, if fluid mobility is sufficiently high for pressure equilibration to occur.

As was stated above, the equality of frame and saturated shear moduli (equation 16) is not an assumption, it is a consequence of the Gassmann theory. This does not mean that it is appropriate to assume that gas sands and brine sands have the same shear modulus. In practice, they represent different pieces of rock from different locations that may have been different from the moment of deposition, and that certainly have undergone different diagenetic histories while they contained different pore fluids. Cementation and other types of diagenesis can be radically different and may result in different porosities and degrees of cementation, as well as in very different frame moduli. In fact, we must revisit the entire idea of fluid substitution as being a good way to determine the dependence of rock moduli on fluid type. The instantaneous mechanics of Gassmann's equations are correct, but it is probably erroneous to ignore geochemical and other factors that may become significant over geologic time.

Using Gassmann's equations

We assume that V_P, V_S, and porosity are known at a given saturation. V_S may be measured or estimated from a V_P-V_S relationship. Given solid and fluid densities, the bulk density is determined from the mass-balance equation 3 above.

Greenberg and Castagna (1992) developed a method for predicting shear-wave velocity in porous sedimentary rocks. The method couples empirical relations between V_P and V_S with Gassmann's equations and accounts for mixed lithologies and fluids. V_S can be estimated from V_P in multimineralic, brine-saturated rocks on the basis of empirical V_P-V_S relations in pure monomineralic lithologies, by using arithmetic and harmonic means of the constituent pure-lithology predicted shear velocities. It is given as

$$V_S = \frac{1}{2}\left\{\left[\sum_{i=1}^{L} X_i \sum_{j=0}^{N_i} a_{ij} V_P^j\right] + \left[\sum_{i=1}^{L} X_i \left(\sum_{j=0}^{N_i} a_{ij} V_P^j\right)^{-1}\right]^{-1}\right\}$$

and

$$\sum_{i=1}^{L} X_i = 1, \tag{17}$$

where L is the number of monomineralic lithologic constituents, X_i are the volume fractions of lithologic constituents, a_{ij} are the empirical regression coefficients, and N_i is the order of the polynomial for constituent i.

One can then estimate V_S from measured V_P for other fluid saturations by using Gassmann's equation in an iterative manner. The method consists of iteratively locating a point (V_P,V_S) on the brine relationship that transforms, by using Gassmann's equation, to the measured V_P and unknown V_S for the new fluid saturation.

Figure 6 shows that the Raymer-Hunt-Gardner equation yields a V_P-V_S trend that is in almost perfect agreement with Greenberg and Castagna's (1992) sandstone V_P-V_S trend and the resulting trend obtained by combining Gassmann's equations with a frame Poisson's ratio of 0.1.

The saturated bulk and shear moduli are then obtained from equations 18 through 21:

$$V_P = \sqrt{\frac{\kappa_{sat} + \frac{4}{3}\mu_{sat}}{\rho_b}} \tag{18}$$

$$\kappa_{sat} = \rho_b V_P^2 - \frac{4}{3}\mu_{sat} \tag{19}$$

$$V_S = \sqrt{\frac{\mu_{sat}}{\rho_b}}, \tag{20}$$

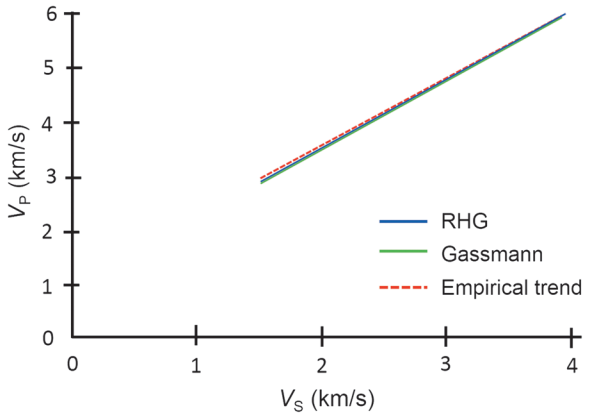

Figure 6. V_P-V_S relationships in sandstone from the Raymer-Hunt-Gardner equation ("RHG," blue line), Gassmann equations that use a frame Poisson's ratio of 0.1 (green line), and an empirical V_P-V_S trend for sandstones (dotted red line). The trends are virtually identical.

$$\mu_{sat} = V_S^2 \rho_b. \tag{21}$$

Equations 18 and 20 are the velocity equations for elastic waves propagating in elastic media. In reality, however, porous rocks are not strictly elastic. Seismic waves are thus attenuative and dispersive, and the velocity equations are more complicated (Biot, 1956). We will assume that it is safe to use equations 18 and 20 at seismic frequencies. However, it is debatable how applicable they are at sonic and ultrasonic frequencies, especially in low-permeability rocks.

Usually, laboratory measurements help us to estimate the rock-frame bulk and shear moduli, the grain density, the porosity, and the fluid bulk modulus. When lab data are not available, well logs and rock-physics relationships are used to determine the input parameters for Gassmann's equations. Elastic bounds can be used to determine the effective elastic moduli for rocks composed of different constituent layers and minerals.

To understand the different properties of rocks, we need information with respect to (1) the fraction, by volume, of various constituents, (2) elastic moduli of various phases, and (3) geometric details of how phases are arranged relative to one another (Avseth et al., 2005).

In practice, it is difficult to specify the internal geometry. If we just have information on the volume fraction of the constituents and their elastic moduli, we can only predict the upper and lower bounds of the elastic moduli and velocities of the composite rocks.

Voigt (1928) suggests the stiff upper bound of the effective elastic moduli. The upper bound describes an isostrain situation, because the strain is equal in all of the columnar layers (Figure 7a). The stress must, therefore, be different in each constituent layer. The Voigt upper bound on the effective elastic modulus of a mixture of N material phases is

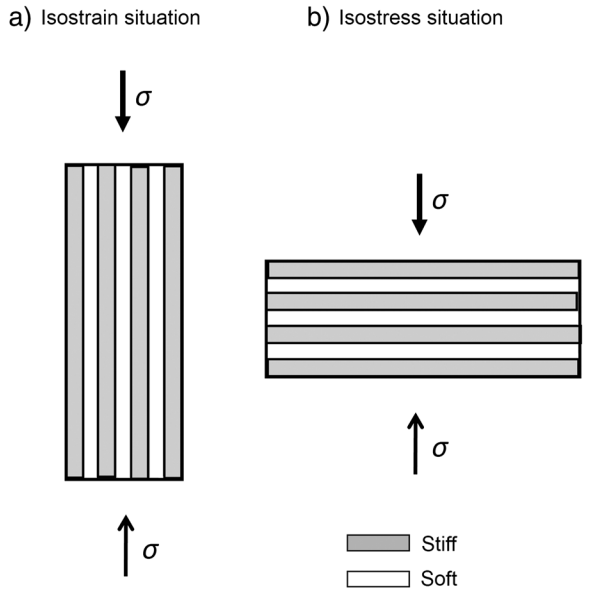

Figure 7. Sketch showing the stress-strain situation in effective media leading to the bounds of (a) Voigt and (b) Reuss. Here, σ is the compressive stress.

$$M_V = \sum_{i=1}^{N} f_i M_i, \tag{22}$$

where f_i is the volume fraction of the ith constituent and M_i is the elastic modulus of the ith constituent.

Reuss (1929) gives the soft lower bound of the effective elastic moduli (Figure 7b). The lower bound describes the isostress situation, because Reuss assumed that the stress applied to each of the constituent layers is the same, but the strain is different. Compressible layers will be more deformed by the compressive stress than stiff layers will. The Reuss lower bound is given as

$$\frac{1}{M_R} = \sum_{i=1}^{N} \frac{f_i}{M_i}, \tag{23}$$

where M can represent any modulus — bulk or shear — and the subscript R designates Reuss.

Hill (1963) shows that when the shear modulus is the same in all of the constituents, the modulus of the mixture is the arithmetic average of the Voigt and Reuss bounds. That average is generally used to calculate effective matrix properties and works well when shear moduli are similar. However, it is likely to be significantly in error when soft and hard components are combined (e.g., quartz and clay). Thus, when the mineralogy is known for a rock, the Reuss-Voigt-Hill average can be used to calculate effective bulk and shear moduli, as

$$M = \frac{1}{2}(M_V + M_R), \tag{24}$$

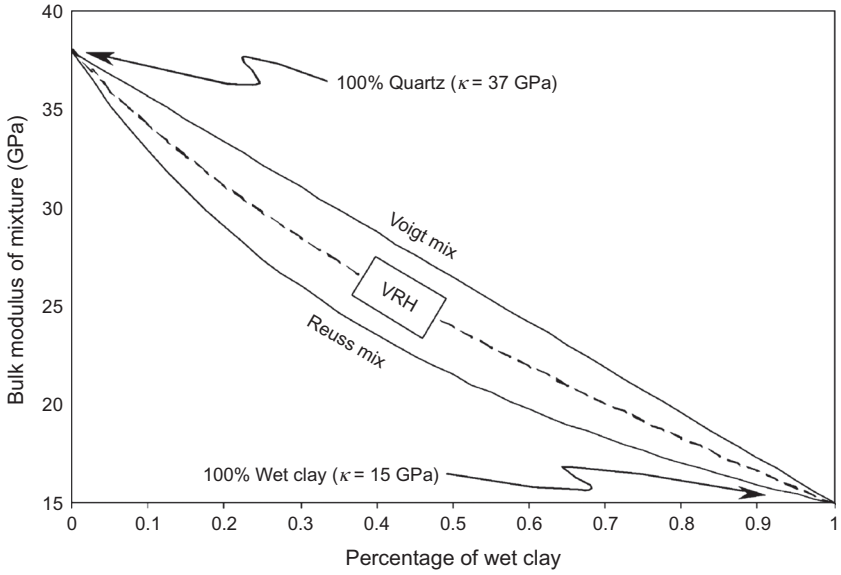

Figure 8. Bulk modulus of a mixture plotted as a function of the fraction of wet clay, showing the "stiff" Voigt and "weak" Reuss bounds calculated for pure quartz and wet clay. The VRH average is simply the average of the Voigt and Reuss bounds. After Figure 1 of Smith et al. (2005). Used by permission.

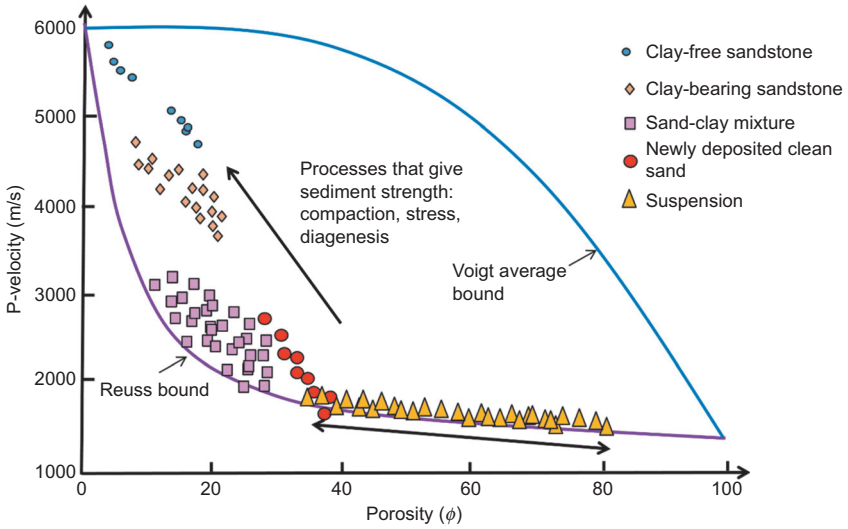

Figure 9. P-wave velocity plotted as a function of porosity for a variety of water-saturated sediments, compared with the Voigt and Reuss bounds. Data from Yin (1992), Han (1986), and Hamilton (1956). After Figure 1.6 of Avseth et al. (2005). Copyright Cambridge University Press. Reprinted with permission.

where M is the effective grain modulus, which can be bulk or shear, and subscripts V and R designate Voigt and Reuss, respectively. The medium is assumed to be isotropic, linear, and elastic. Figure 8 shows the Voigt and Reuss bounds calculated for pure quartz and wet clay mixtures.

Wood's (1941) equation is identical to the Reuss bound and is used to estimate the effective bulk modulus of the pore fluid (κ_f).

As was stated previously, when the geometries of the constituents are not known, the Voigt and Reuss averages give us the upper and lower extreme values of the bounds. Values for other sediment situations fall within those bounds. That can be understood in the overall context as follows.

If we plot the variation of P-wave velocity of, for example, water-saturated sediments that range from ocean-bottom suspensions to consolidated sandstones, we will probably get something similar to what is shown in Figure 9. A few observations are in order.

- When the particles are suspended in water, their acoustic properties must fall on the Reuss average of mineral and fluid moduli.
- When particles are deposited on the water bottom, their properties still lie on or slightly above the Reuss average, as long as they are weak and unconsolidated. The porosity of these particles will depend on the geometry of the particle stacking. Clean, well-sorted sands will be deposited with porosities near 40%. Poorly sorted sands will have lower porosities and will be deposited along the Reuss bound (Figure 9). Chalk will be deposited at a high initial porosity of 55% to 65%. Shales can have even higher initial porosities. As those sediments get buried, different processes set in — such as effective stress, compaction, and cementing — and these processes move the sediments off of the Reuss bound. The porosity at which the rock starts to become lithified and develop rigidity is called the *critical porosity* (ϕ_c).
- With increasing diagenesis, the moduli move farther above the Reuss bound.
- Sometimes the bounding methods are not seen as being very helpful as the upper and lower bounds are well separated between the end members. In such cases, the critical porosity seems to help because it separates the fluid-bearing suspensions from the load-bearing frame.

Hashin-Shtrikman bounds can be used to calculate the narrowest possible range for the bulk and shear modulus components, and those bounds are different for the two moduli. They would, therefore, lie within the Voigt and

Reuss bounds. The Hashin-Shtrikman bounds physically represent the cases of the medium being completely filled by concentric spheres of the constituent materials. The upper bound corresponds to the case of the softer material occupying the interior spheres; conversely, the lower bound corresponds to the softer material occupying the outer spheres. For the case of one of the materials being fluid, it can be seen from the equation below that the upper bound corresponds to the case of equant porosity and the lower bound reduces to the Reuss bound (i.e., to a suspension). These bounds are sufficiently wide to accommodate all of the intermediate pore structures, including fractures.

If mineral 1 is stiffer than mineral 2, the upper Hashin-Shtrikman bounds are given as

$$\kappa_{HS} = \kappa_1 + \frac{f_2}{(\kappa_2 - \kappa_1)^{-1} + f_1\left(\kappa_1 + \frac{4}{3}\mu_1\right)^{-1}}, \quad (25)$$

$$\mu_{HS} = \mu_1 + \frac{f_2}{(\mu_2 - \mu_1)^{-1} + \frac{2f_1(\kappa_1 + 2\mu_1)}{5\mu_1\left(\kappa_1 + \frac{4}{3}\mu_1\right)}}. \quad (26)$$

In these equations, κ_1, κ_2 are the bulk moduli for the constituent phases, μ_1, μ_2 are the shear moduli for the constituent phases, f_1, f_2 are the volume fractions for the constituent phases, ϕ is porosity, and the subscript HS represents Hashin-Shtrikman bounds.

The lower bounds can be computed by reversing the order of the two minerals in the equations.

Estimating κ^*

Usually, the bulk modulus of the rock-frame skeleton is unknown, and a variety of empirical equations to estimate the frame bulk modulus can be applied. The problem with this approach is that the empirical estimates of the frame modulus may be inconsistent with the observed velocities. Keep in mind that the frame modulus is the modulus measured at irreducible saturation, so the rock frame likely has interacted chemically with the wetting fluid. Thus, in fluid substitution, the "wetted" frame bulk moduli should be used. The use of laboratory measurements of dry-rock moduli usually results in incorrect fluid substitutions, unless the measurements are made under appropriately "humid" conditions (Smith et al., 2003; included on the USB flash drive).

For this reason, a common approach is to use in situ well-log measurements, in rocks of known saturation and fluid content, to calculate the frame modulus by inverting Gassmann's equations:

$$\kappa^* = \frac{\kappa_{sat}\left(\frac{\phi\kappa_0}{\kappa_f} + 1 - \phi\right) - \kappa_0}{\frac{\phi\kappa_0}{\kappa_f} + \frac{\kappa_{sat}}{\kappa_0} - 1 - \phi}. \quad (27)$$

Unfortunately, errors in the parameters on the right side of equation 27 likely cause the inverted frame modulus to be erroneous, and they can in fact be negative, even when what appear to be physically reasonable parameters are used. Thus, it is always necessary to check for negative frame moduli and Poisson's ratios when using equation 27.

Another method for calculating κ^* is to use V_P and V_S to determine the frame shear modulus and then to calculate the frame bulk modulus from an assumed frame Poisson's ratio (Gregory, 1977; included on the USB flash drive). This method is preferred in clean sandstones for which it is safe to assume a Poisson's ratio of approximately 0.1 (Castagna et al., 1985; Castagna et al., 1993). In shaly sandstones, the frame Poisson's ratio must be increased according to the shale content (Smith et al., 2003; included on the USB flash drive).

The fluid-substitution paradox

If we consider a given rock frame with two different fluids or fluid mixtures in the pore space, exhibiting two different effective fluid moduli, κ_{f_1} and κ_{f_2}, equation 14 can be written twice for the two corresponding saturated moduli, κ_{sat_1} and κ_{sat_2}, and subtracted to eliminate the constant frame modulus. This yields

$$\frac{\kappa_{sat_2}}{\kappa_0 - \kappa_{sat_2}} - \frac{\kappa_{sat_1}}{\kappa_0 - \kappa_{sat_1}} = \frac{\kappa_{f_2}}{\phi(\kappa_0 - \kappa_{f_2})} - \frac{\kappa_{f_1}}{\phi(\kappa_0 - \kappa_{f_1})}. \quad (28)$$

Upon first inspection of equation 28, it appears that the change in saturated modulus is independent of the frame modulus. This runs counter to the idea that compressible rock frames have a larger fluid-substitution effect than incompressible rock frames have. The solution to the paradox, of course, is that the frame modulus is contained implicitly in the saturated moduli. When the frame modulus is small, the corresponding saturated moduli are also small, and the fluid-substitution effect is large. Rearranging equation 28 gives

$$\kappa_{sat_2} = \frac{\kappa_0\left[\frac{\kappa_{sat_1}}{\kappa_0 - \kappa_{sat_1}} - \frac{\kappa_{f_1}}{\phi(\kappa_0 - \kappa_{f_1})} + \frac{\kappa_{f_2}}{\phi(\kappa_0 - \kappa_{f_2})}\right]}{1 + \left[\frac{\kappa_{sat_1}}{\kappa_0 - \kappa_{sat_1}} - \frac{\kappa_{f_1}}{\phi(\kappa_0 - \kappa_{f_1})} + \frac{\kappa_{f_2}}{\phi(\kappa_0 - \kappa_{f_2})}\right]}. \quad (29)$$

Thus, fluid substitution can be performed without explicitly using frame moduli.

Fluid properties

Pore fluids have highly variable fluid moduli and densities that are strongly dependent on pressure, temperature, and composition (Batzle and Wang, 1992). Although the Batzle and Wang equations have been continuously updated since their first publication, as more calibration points have become available, the general conclusion that these factors must be taken into consideration when one is selecting fluid moduli for Gassmann's equations remains intact. Figure 10 shows the ranges of fluid moduli from the Batzle and Wang equations, as a function of temperature and for a wide range of pore pressures and compositions (the ranges of moduli for each fluid type include the effects of variations of gas density for gases, API gravity and gas-oil-ratio for oils, and salinity for brines, as well as the range of pressures encountered in petroleum exploration). It is important to note that saline brines can have a significantly higher modulus than the typical value of 2.5 GPa that is commonly used, and in those cases the contrast with hydrocarbons is enhanced. As a general rule, oil moduli are between brine and gas moduli and, as temperatures increase, become more similar to gas moduli.

Saturated versus frame moduli

For given solid and fluid moduli, Gassmann's equations can be used to determine the relationship between frame and saturated moduli at any constant porosity. As is shown in Figure 11 for sandstones, the constant-porosity lines converge at the solid-grain modulus, but they also converge toward high porosities. For high frame moduli, there is little porosity dependence. For low frame moduli, the variation of saturated modulus with porosity increases. However, such low frame moduli generally are associated with high porosities where the lines converge, and the greatest deviations would be associated with very unusual porosities. Using a frame Poisson's ratio of 0.1 allows Figure 11 to be converted into a V_P-versus-V_S crossplot (Figure 12). The convergence of the constant-porosity trends at high porosities is increased, so that there is little difference between the 30% and 100% porosity lines. Thus, the 100% porosity line serves as a very useful lower bound for V_P/V_S over the entire range of velocities. The 100% porosity line on a V_P-V_S crossplot is only slightly below the observed empirical relationships in sandstones (Figure 12), suggesting that natural processes tend to minimize Poisson's ratio. Notably, we find that abnormally high V_P/V_S values occur for low-velocity rocks with abnormally low porosities. Without the need for inclusion modeling, we can conclude, then, that liquid-filled naturally fractured

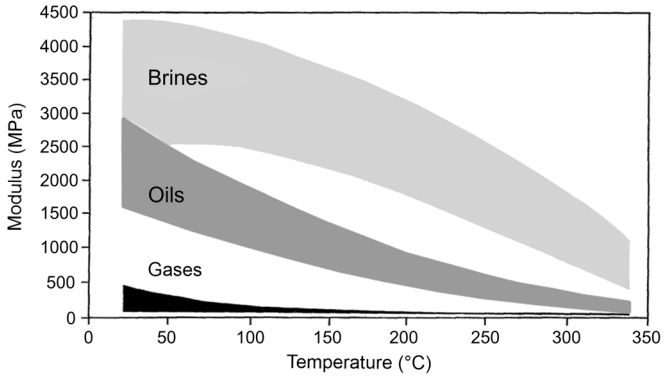

Figure 10. Pore-fluid moduli versus temperature for the range of pore pressures and compositions commonly found in exploration applications, using the Batzle and Wang (1992) equations.

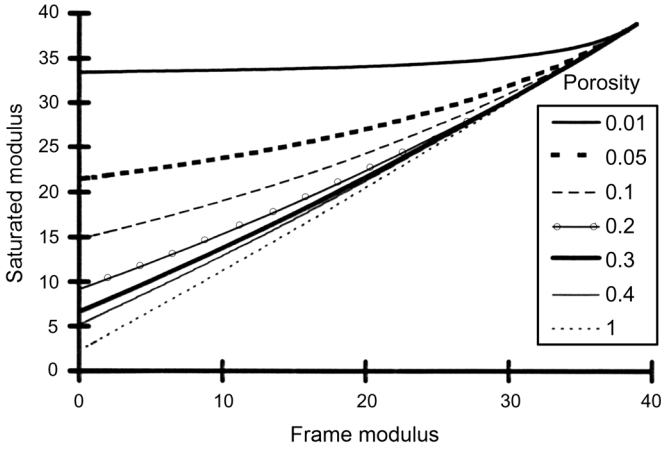

Figure 11. Saturated modulus versus frame modulus for sandstones of various porosities and a fluid modulus of 2.5 GPa (brine).

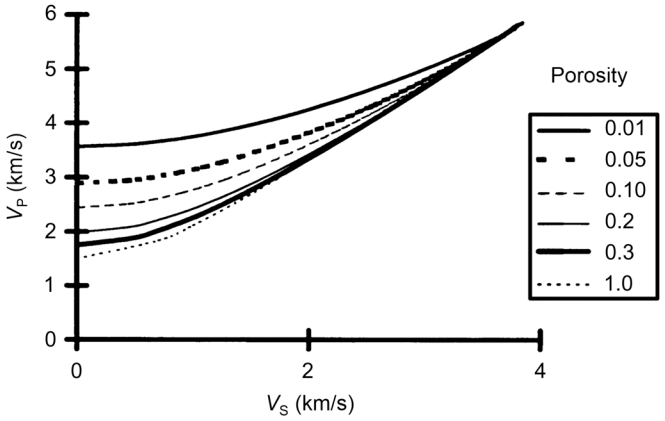

Figure 12. V_P-V_S constant-porosity curves from Gassmann's equations, assuming a frame Poisson's ratio of 0.1.

rocks should exhibit abnormally high V_P/V_S values relative to empirical V_P-V_S trends.

Low gas saturations

Figure 13 shows a typical Gassmann fluid-substitution curve for an unconsolidated sandstone. Most of the velocity change occurs with the first few percentages of gas saturation. In such situations, it is difficult to distinguish low gas saturations from commercial ones. This is a fundamental limitation of direct hydrocarbon detection using seismic amplitudes. In deeper reservoirs, the rock frame is typically stronger and the gas modulus is larger, so the partial-saturation effect may not be as pronounced (Han and Batzle, 2002) (Figure 14). The saturation curves in this particular case are for pressures corresponding to depths of 1000 ft (Figure 14a) and 20,000 ft (Figure 14b).

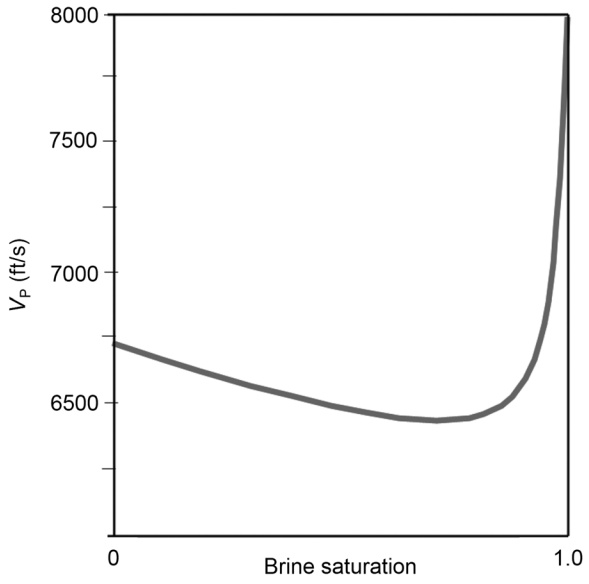

Figure 13. Gassmann P-wave-velocity fluid-substitution curve for a shallow, unconsolidated, 29%-porosity sandstone and light dry gas. Solid modulus = 38 GPa; brine modulus = 2.5 GPa; gas modulus = 0.05 GPa.

Sensitivity and uncertainty

As was previously discussed, at low porosities Gassmann's equations predict an extremely large change in saturated modulus with a small change in porosity. Figure 15 shows, quantitatively, the magnitude of that effect. Note that greater porosity sensitivity occurs at smaller frame moduli.

The process of fluid substitution using Gassmann's equations has many input parameters that are not perfectly known. Those parameters include V_P, V_S, density, porosity, matrix density, solid-grain bulk modulus, original water saturation, water density, brine modulus, hydrocarbon density, hydrocarbon modulus, and new water saturation. Castagna et al. (1993) determined from repeated logging runs that the precision of "good" P-wave sonic-log velocities is approximately 2% and that for shear-wave velocities is on the order of 5%.

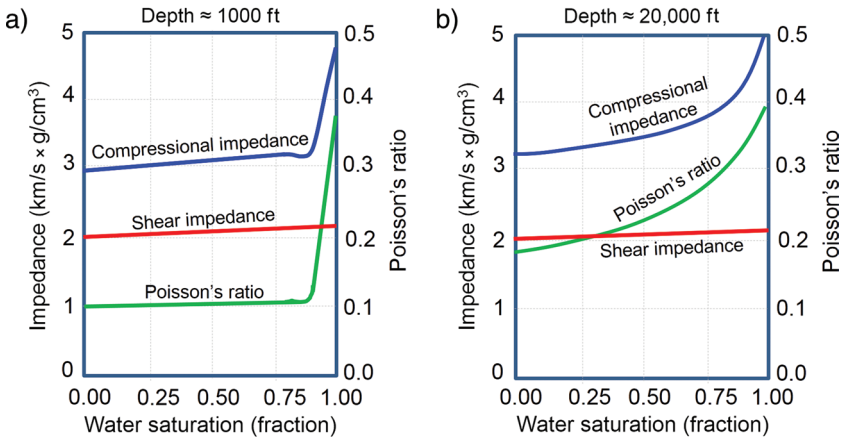

Figure 14. Seismic impedance versus water-gas saturation for (a) a shallow sandstone reservoir at 1000 ft and (b) a deep sandstone reservoir at 20,000 ft. The drop in impedance with the addition of the first few percentage points of gas saturation is less pronounced in deep reservoirs. After Figure 9 of Han and Batzle (2002). Used by permission.

Accuracies are another matter, and, even when the measurements are repeatable, they can be very wrong for a variety of reasons (see Castagna et al., 1993, for a detailed discussion). Density logs have even more serious accuracy problems, and one might safely assume that "precise" means precisely wrong, unless there is reason to believe otherwise. Borehole gravity measurements can be more accurate, but they have limited vertical resolution and are only infrequently available. If rock composition is not perfectly known, matrix properties such as density and modulus can vary significantly. Porosity commonly is not known to better than ±2 porosity units. For example, for a calculated porosity of 10%, the true porosity might, with good probability, be anywhere between 8% and 12%. Water-saturation estimates are frequently on the order of 20% in error. When we are predicting velocities in an exploration mode, it is unlikely that the prospect's water saturation for the hydrocarbon-bearing scenario will be known to better than ±20%. Fluid densities and moduli are rarely known precisely.

Such errors and uncertainties are propagated through Gassmann's equations and result in significant error bars around predicted velocity changes. Apologists for Gassmann's equations quote small percentage errors in

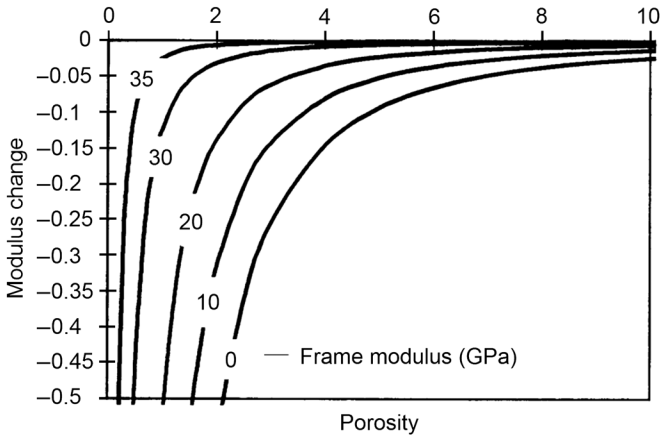

Figure 15. Fractional change in saturated bulk modulus ($\Delta\kappa/\kappa$) from brine to gas as a function of frame modulus and porosity. Solid grain modulus = 38 GPa; brine modulus = 2.5 GPa; gas modulus = 0 GPa.

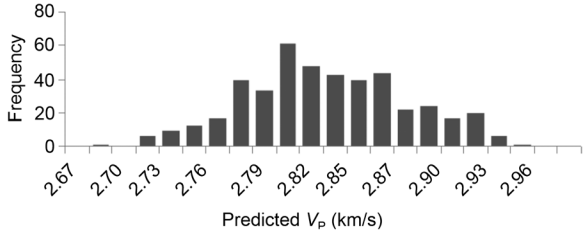

Figure 16. Output histogram from stochastic fluid substitution for an unconsolidated sandstone, by using the parameters in Table 1. The input V_P is 3.0 km/s and the deterministic Gassmann result is 2.81 km/s. The range of stochastic outputs is as large as the deterministic change in velocity.

predicted velocities. Unfortunately, a "small" percentage error in the predicted velocity is often an enormous percentage error in the change in velocity as fluids change — which is, of course, the most relevant quantity of interest for hydrocarbon detection. Indeed, the problem is so severe that it is not meaningful for explorationists to speak of "the" brine-sand or gas-sand model; rather, a probability density function of outcomes should be considered.

Figure 16 is the result of stochastic fluid substitution for a typical unconsolidated sand. It is the histogram of predicted gas-sand V_P for fluid substitution from brine sand. More than 400 trials were conducted with the input parameters being perturbed randomly (as would result from uncorrelated errors) by using a uniform distribution over an assumed range of uncertainty (given in Table 1). The spread in the output histogram is as wide as the predicted change in velocity. Figure 17 is a quality-control histogram that shows that this spread is not related to nonphysical frame moduli being inverted from Gassmann's equations, but instead is entirely the result of a propagation of errors. Similarly, the implied frame Poisson's ratios are all physically reasonable. In the case of well-lithified sandstones, where the fluid substitution effect is smaller,

Table 1. Input parameters for stochastic fluid substitution using Gassmann's equations in an unconsolidated sandstone. The exact Gassmann fluid substitution is 2.81 km/s.

Parameter	Parameter value	Range
V_P	3.00 km/s	2%
V_S	1.41 km/s	2%
Porosity	30%	2 P.U.
Grain density	2.65 g/cm^3	0.2 g/cm^3
Grain modulus	38 GPa	2 GPa
Water saturation	100%	0%
Water density	1.05 g/cm^3	0.05 g/cm^3
Water modulus	2.5 GPa	0.25 GPa
Gas density	0.1 g/cm^3	0.1 g/cm^3
Gas modulus	0.1 GPa	0.05 GPa
New saturation	30%	20%

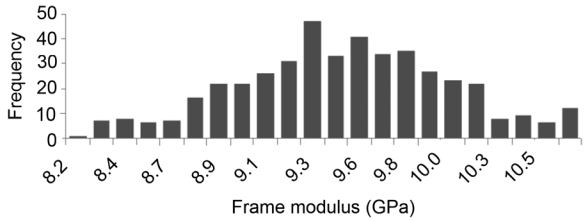

Figure 17. Histogram of inverted frame moduli for the stochastic fluid substitution shown in Figure 16.

the error can be many times the deterministic predicted change in velocities. It is clear that Gassmann's equations, even if theoretically applicable to real world problems in some cases, must be taken with a grain of salt.

Differences in frame modulus from inverted modulus and between brine and gas sands

Differences between inverted and actual frame moduli are most severe in laboratory measurements, for which the wetting fluid may change, different rock samples may be used, or the same sample may change its frame properties during the course of various experimental runs as pressure is increased and decreased several times. Figure 18 shows a typical disagreement between laboratory measurements and Gassmann's predictions (in this case the difference is too large to be explained by dispersion). Differences such as these are attributed to frame hardening or softening relative to the dry rock. That is because when water is added to the dry rock, the water can react chemically or physically with the mineral components of the rock (particularly with clays). For example, water can form a silica gel around quartz grains, causing the grains to repel each other and

weaken the frame at a low effective stress. Water can also lubricate the frame by causing structural clays to lose rigidity. Alternatively, water can harden or soften the frame by causing clays to swell, thereby binding the other mineral components more tightly, or by reducing the frame modulus as the clays become more compressible. Such effects are very dependent on the rock mineralogy (clay type and structural position) and the salinity and pH of the pore fluid. None of these effects is considered in Gassmann's equations.

Another situation in which care must be taken to use the proper frame moduli is when information from an existing well is used to model how seismic responses will change, away from a well, as fluid content changes, particularly in another trapping location. When different pieces of the same rock formation are saturated with differing pore fluids over geologic time, there may be differences in their diagenetic history. There is a school of thought among geophysicists that claims porosity is better preserved in oil reservoirs than in the downdip fully brine-saturated rocks. This is not a universally accepted fact, particularly among knowledgeable geologists (A. Brown, personal communication, 1989), but the possibility must be considered unless there is evidence to the contrary. Differing diagenetic histories or not, in an exploration mode, brine-filled and hydrocarbon-bearing sands occur at different spatial locations and possibly at different stratigraphic positions. Thus, some difference in rock-frame properties between brine sands and gas sands is to be expected, if only from natural variations in the geology. The velocity in an actual gas sand may, therefore, differ greatly from the velocity predicted from the corresponding brine sand by using Gassmann's equations. If the brine sand and gas sand have different pore pressures, or if the brine sand is far downdip and is under a different confining pressure, differences in frame moduli are to be expected. In a time-lapse mode, pressure changes with production may result in rock-frame properties that vary continuously with time.

Figure 19 shows a seismic section over a producing oil field that exhibited a bright spot where the seismic data were acquired about 15 years after production began. The original oil-water contact can still be seen on the seismic, although the water level has risen significantly over the years. The sand thins updip and loses amplitude as it pinches out. By the time this vintage of seismic data was acquired, a significant gas cap had developed. The gas-water contact is not obvious on the seismic amplitudes. The fact that the seismic data acquired after production seem to be responding to the original water level and not to the contemporaneous oil-water or gas-oil contacts is curious.

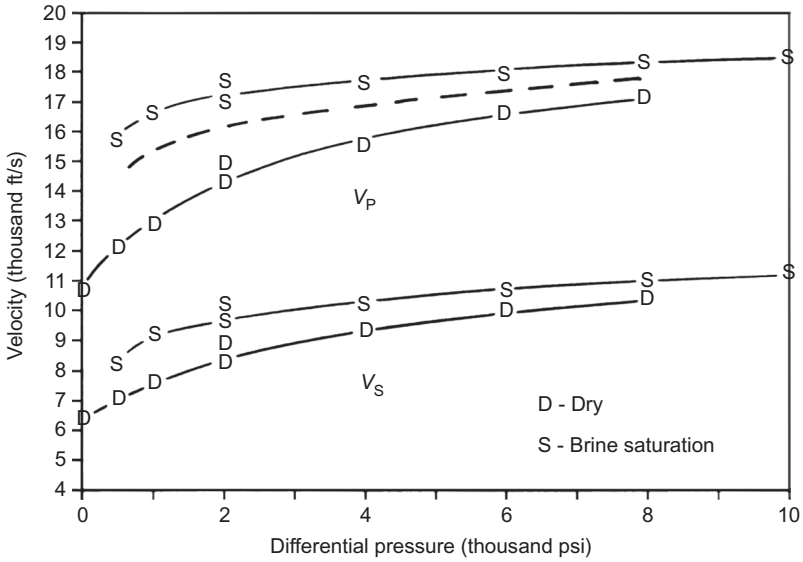

Figure 18. Laboratory-measured brine-saturated and dry compressional-wave and shear-wave velocities in a well-lithified calcareous sandstone. The dashed line is the Gassmann-equation predicted V_P given the dry V_P and V_S values. Note that according to Gassmann's equations, the water-saturated V_S should have been lower than the dry V_S; note also that the water-saturated V_P is significantly higher than the Gassmann prediction. Figure courtesy of M. Batzle. Used by permission.

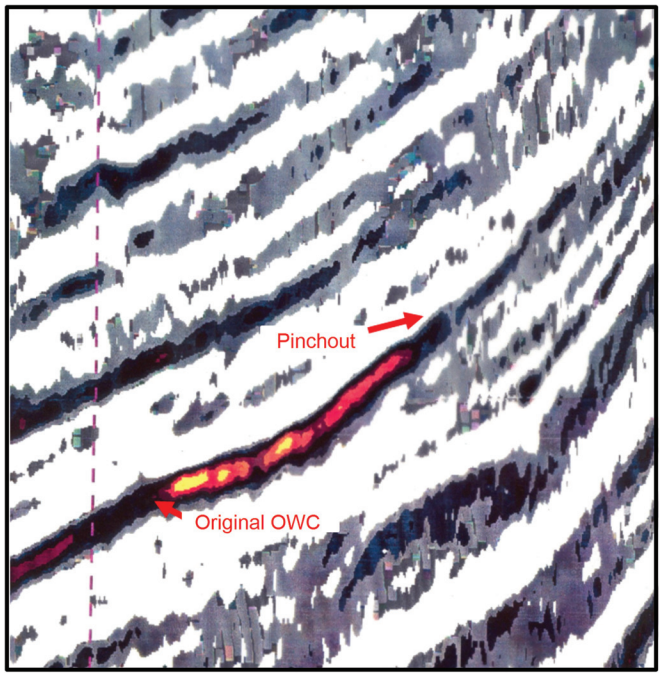

Figure 19. Relative-amplitude-processed poststack 3D migrated section showing an oil-reservoir bright spot. Only negative amplitudes are shown. Yellow is the strongest negative amplitude. The sandstone increases in thickness downdip and pinches out updip. A clear amplitude increase at the original oil-water contact follows structural contours. The oil-water contact and gas-oil contact from the time that the seismic data were acquired are not evident. It is believed that the amplitudes here are controlled primarily by thickness and porosity, with hydrocarbon effects being secondary.

The fact that residual oil remains is one possible explanation, but the oil properties here are closer to brine properties than to gas properties. Furthermore, the lack of an amplitude change associated with the gas-oil contact needs an explanation. One possibility is that there is a dominant porosity overprint on the amplitudes, in addition to the hydrocarbon effect, and the rock is higher porosity wherever the oil was originally in place. That is little more than conjecture at this point, however, and a systematic study using reliable porosity information in wells is needed to resolve the issue on a case-by-case basis.

Alternatives to Gassmann's equations

Given the uncertainties and violated assumptions of Gassmann's equations, the question must be asked regarding whether a given Gassmann prediction should be believed, or is in fact superior to several alternative approximate fluid-substitution schemes. Approximations are generally easier to apply and require less input, but at the same time they have fewer parameters and are consequently more robust. Some of those alternatives follow.

- Raymer-Hunt-Gardner (RHG) equation. It is apparent from the RHG equation (equation 5) that a crude form of fluid substitution can be accomplished by modifying the fluid velocity (i.e., stretching the RHG equation well beyond its range of calibration). It does at times produce reasonable answers.
- Mavko et al. approximation. Mavko et al. (1995) proposed replacing the bulk modulus in Gassmann's equations with the plane-wave modulus (M) (the same as the P-wave modulus). This has the advantage of being directly calculable from P-wave velocity and density, without requiring explicit knowledge of the shear modulus. Mavko et al. (1995) conclude that the method is accurate to within 3% of the original velocity.
- Castagna et al. approximation. This is the simplest approximation and requires only a single input parameter. It is the relationship between brine-sand and gas-sand P-wave velocities, as given by Castagna et al. (1993). The equation is

$$V_{\text{gas sand}} = -0.07V^2_{\text{brine sand}} + 1.67V_{\text{brine sand}} - 1.74 \text{ km/s}. \quad (30)$$

  Figure 20 shows an example of the errors of the Mavko et al. and Castagna et al. (i.e., quick-estimate) approximations relative to the exact Gassmann prediction (assuming that it is correct).
- V_P-V_S relationships: A simple way to perform fluid substitution, starting with brine-saturated rock replaced with light dry gas, is to predict V_S from V_P, correct V_S for density as the fluid changes, and then recompute V_P assuming a rock-frame Poisson's ratio.

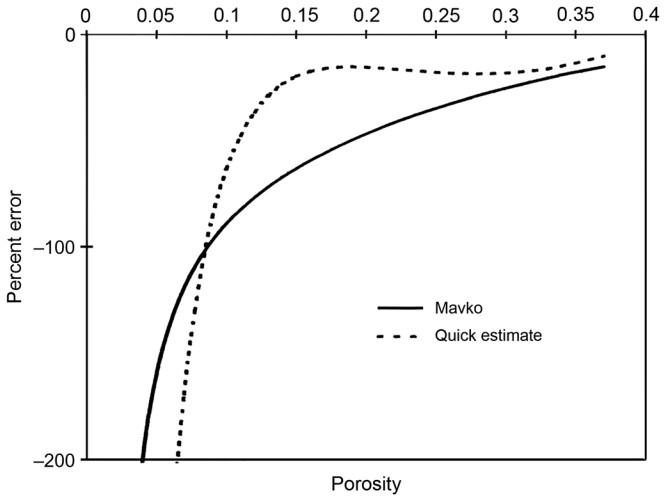

Figure 20. Percent error in the predicted change in velocity relative to the Gassmann prediction as gas is substituted for brine in sandstones that obey the Raymer-Hunt-Gardner P-wave velocity-porosity transform. The solid line is the Mavko et al. approximation, and the dashed line is the quick-estimation technique of Castagna et al. (1993), as given by equation 30. The gas modulus is taken to be zero and the brine modulus is 2.5 GPa.

Recommendations for practical fluid substitution

The limitations of Gassmann's equations are clear, but in the final analysis, they remain the theoretical basis for understanding the difference between brine-sand and gas-sand velocities and for justifying V_P-V_S relationships for brine-saturated sandstones. In practice, one may wish to use one of the less exact, but perhaps more robust, methods discussed above, at least as a rough estimate to check the quality of the predictions made. In addition, one needs to be cognizant of such issues as frame-modulus variation between gas sands and brine sands, and of the uncertainty in the Gassmann predictions. Certainly, the use of Gassmann's equations in low-porosity rocks must be viewed with great suspicion. Nevertheless, fluid substitution is a necessary aspect of interpreting seismic-amplitude and AVO anomalies. If the task must be performed, it might as well be done correctly. General considerations for performing a practical fluid substitution are as follows.

- It is important to know whether the log data are reading true formation properties. Density logs, if they are in fact reading formation densities, are most certainly measuring the density of the invaded zone. In gas sands, density logs do not measure true formation

density, because of the abnormal electron density of hydrocarbons. Density logs must be environmentally corrected properly in order to provide the true formation density. Sonic logs may or may not be reading formation velocities. If dispersion is significant, and Gassmann's equations overestimate the fluid-substitution effect, the residually gas-saturated flushed zone may in fact demonstrate a higher velocity than the formation does with commercial gas saturation. If that is the case, the sonic-log refraction problem becomes a "hidden-layer" problem, and first breaks will be from the invaded zone rather than from the formation.

- If the sonic-log traveltime is slower than the drilling-mud traveltime, it is unlikely to be correct. Shallow unconsolidated gas sands often exhibit sonic-log readings that are equal to the drilling-mud velocity.
- As a result of free-gas-caused attenuation of the acoustic signal in the borehole and in the formation, and because of poorer coupling of acoustic energy into low-Poisson's-ratio formations, sonic-log readings in gas sands are notoriously unreliable. In fact, sonic-log cycle skipping is often used as a quick-look indicator of gas.
- For the above reasons, brine-sand sonic-log velocities are generally more reliable than gas-sand velocities are. If one is performing fluid substitution, it is better to start with reliable velocities. Thus, it is better to substitute gas into a brine sand than brine into a gas sand.
- Density logs are notoriously susceptible to poor hole conditions. For seismic-modeling purposes, it is generally better to reconstruct a density log from other log information that is less subject to experimental error, and to calibrate that reconstruction in zones where the density log is deemed reliable. In practice, it is very common to simply ignore the density log and replace it with Gardner's equation (Gardner et al., 1974) or with a constant density. When sand and shale velocities are similar, such substitutions result in large errors in shale and sand reflection coefficients.
- When performing fluid substitution in shaly sands, remember that residual-water saturation in gas-bearing zones can be on the order of 50%.

Gas-saturated shales

Although shales are low-permeability rocks, there is no question that free gas exists in shales. It has long been known that most gas is generated in and migrates through shales, that shales have limited seal capacity, and that microseepage of gas above reservoirs generally occurs. Gas chimneys and low-velocity zones are often attributed to such a phenomenon. Today, shales are viewed as being unconventional reservoir rocks so the issue is moot. In everyday exploration practice, however, fluid substitution is rarely performed in shales. One reason is that Gassmann's assumptions are violated in most shales. Clearly, for AVO applications, one should be concerned about the V_P/V_S values in shales above prospective reservoirs. If gas is present, one would expect some reduction in the V_P/V_S value, and that could impact the magnitude of the AVO anomaly because the contrast with gas-bearing reservoir would be reduced. Figure 21 shows acoustic-log V_P and V_S measurements in a gas-bearing shale above a producing reservoir. The V_P/V_S values are suppressed compared with the brine-saturated (wet) shale V_P-V_S trend. However, they are not as low as would be predicted by Gassmann's equations. The shale is less compressible than predicted by Gassmann because the pore-fluid pressure has not had time to equilibrate and consequently the rock is stiffer. Thus, we consider the Gassmann result to be a lower bound on the shale velocity. We should note that the more porous and permeable the shale is, the more valid Gassmann's equations can be, and the closer we can expect velocities to be to the Gassmann prediction.

Figure 22 compares shallow high-resolution multicomponent VSP measurements of V_P and V_S in mixed shales and poor-reservoir-quality sands over a producing reservoir and also off structure. The V_P/V_S values are clearly suppressed above the reservoir, where gas microseepage

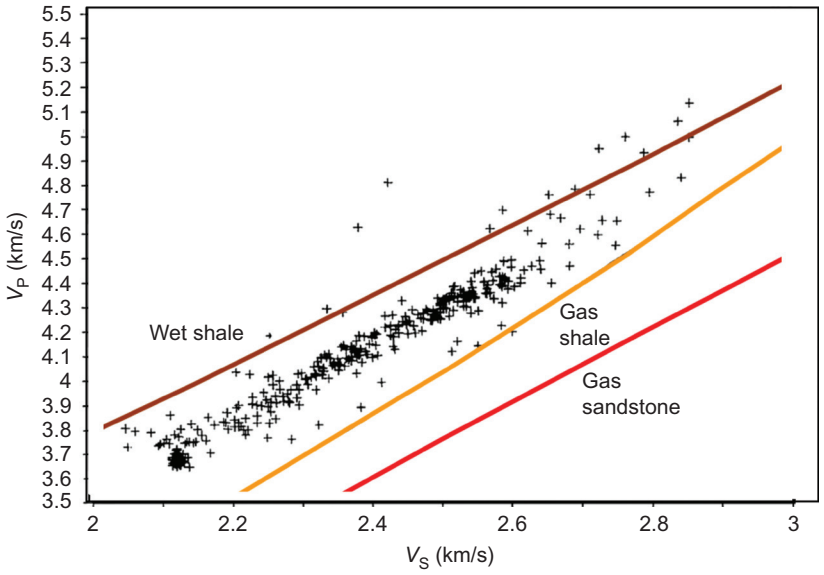

Figure 21. Acoustic-log measurements of V_P and V_S in a gas-bearing shale over a producing gas reservoir. The wet-shale trend and gas-sandstone trend are local empirical trends. The gas-shale trend is computed from the wet-shale trend by using Gassmann's equations.

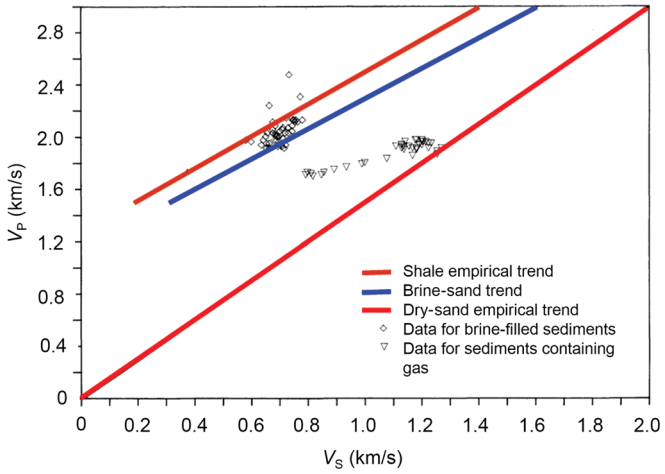

Figure 22. Shallow high-resolution VSP measurements of V_P and V_S over a producing field (inverted triangles) where the sediments are presumed to contain microseeping gas (shot holes could be ignited with matches) and also off structure where the sediments are believed to be completely brine-filled. The brine-saturated V_P-V_S trends are local empirical relationships that are similar to global trends. The dry-sand trend is from Castagna et al. (1985).

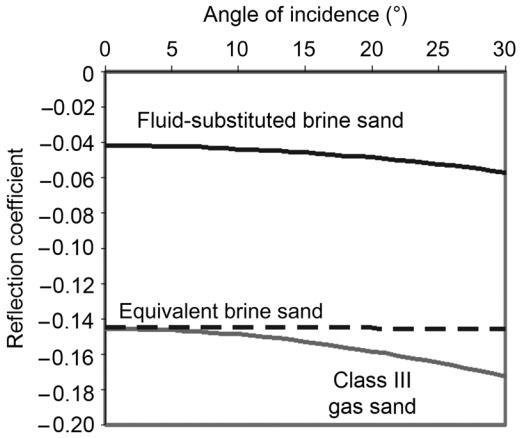

Figure 23. AVO curves for a class 3 gas sand (light-gray solid line), the fluid-substituted brine sand (dark-gray solid line), and the equivalent brine sand with the same AVO intercept as that of the gas sand (dashed line). The AVO gradient distinguishes the two cases.

is presumed to be. The increased shear velocity over the field relative to that of brine-filled rocks off structure is believed to result from increased precipitation of cements caused by bacteria feeding on microseeping gas.

Equivalent versus fluid-substituted sands

Figure 23 compares AVO curves for a class 3 gas sand (defined later) and a fluid-substituted brine sand. Note that they have similar gradients. Because their gradients are similar, the question arises regarding whether the gas sand is in fact an AVO anomaly. The answer, of course, is yes. Had the brine sand had the same AVO intercept that the gas sand did (i.e., that of the equivalent brine sand), its gradient would have been near zero. Thus, we see that the gas sand's AVO response is very anomalous compared with that of the equivalent brine sand. Consequently, in exploration the brine-sand response against which the gas sand should be compared is not necessarily that of the fluid-substituted brine sand.

Table 2. Reasons for Gassmann's equations sometimes failing to be directly applicable for AVO modeling.

1. Violation of assumptions (low permeability, highly compressible mineral components, invasion, dispersion)
2. High sensitivity to input parameters that may be in error
3. Variations in rock-frame porosity and compressibility between gas- and brine-saturated rocks as a result of lateral/vertical geologic variability or differences in diagenesis/cementation caused by different pore fluids
4. Chemical effects at very low effective stress; frame hardening or softening
5. Heterogeneous fluid distribution spatially and between pores of various sizes and shapes; possible inapplicability of Wood's equation
6. The exploration question at hand may not be answered by direct fluid substitution

Conclusions and discussion

We can draw several conclusions that have implications for the influence of rock physics on AVO analysis.

- Precision errors in Gassmann's equations may be larger than the predicted change in velocity.
- Errors in approximations may be within that precision.
- Gassmann's equations can be expected to be most inaccurate in low-permeability and low-porosity rocks. Dispersion and invasion corrections are likely to be important in those cases.
- Observed V_P-V_S relationships agree with Gassmann predictions and potentially can be used to perform fluid substitution more robustly.
- Gas-saturated shales have anomalously low V_P/V_S values, but those values are higher than Gassmann predictions.
- Comparison of gas-sand AVO responses with fluid-substituted brine-sand responses is not necessarily the right exploration approach.

The rock-physics basis for AVO analysis relies on significant empiricism and a bit of theory. Gassmann's equations shed light on the velocity differences between gas sands and brine sands, but the equations are not the entire story and should not be used naively. For a variety of reasons, Gassmann's equations may not be directly applicable to the exploration problem at hand (Table 2). It is important that one take Gassmann predictions with a grain of salt and understand that Gassmann's equations are only applicable to clean, highly permeable reservoir rock. In addition, one should view a single deterministic Gassmann result as only one of many possible stochastic realizations.